

Electronic Supplementary Information for

## **Novel N<sub>6</sub> trisbidentate ligand coordinated Ir(III) complexes and their Ru(II) analogs**

*Li Wang,<sup>a</sup> Peng Cui,<sup>a,b</sup> Bingqing Liu,<sup>a</sup> Svetlana Kilina<sup>a</sup> and Wenfang Sun<sup>a,\*</sup>*

<sup>a</sup>Department of Chemistry and Biochemistry, North Dakota State University, Fargo, North Dakota 58108-6050, United States

<sup>b</sup>Materials and Nanotechnology Program, North Dakota State University, Fargo, North Dakota 58108, United States

## Synthesis

All reagents and solvents were purchased from commercial sources and used as is unless otherwise mentioned.  $^1\text{H}$  NMR spectra were recorded on a Bruker-400 spectrometer in  $\text{CDCl}_3$  with tetramethylsilane (TMS) as internal standard or in dimethyl sulfoxide- $d_6$  ( $\text{DMSO}-d_6$ ). High resolution mass (HRMS) analyses were performed on Waters Synapt G2-Si Mass Spectrometer. Elemental analyses were conducted by NuMega Resonance Laboratories, Inc. in San Diego, California. The corresponding ruthenium precursor *cis*-(phen) $_2$ RuCl $_2$ •2H $_2$ O $^1$  and iridium precursor [Ir(phen) $_2$ OTf $_2$ ]OTf $^2$  were synthesized according to the literature methods. The ligand 3,8-difluorenyl-1,10-phenanthroline (phen-2F $_8$ ) was prepared by Suzuki coupling reaction between 3,8-dibromo-1,10-phenanthroline (phen-2Br) and 2-(9,9-di(2-ethylhexyl)-9H-fluoren-2-yl)-4,4,5,5-tetramethyl-1,3,2-dioxaborolane. $^3$

**Complex 1.** In a 100-mL round bottle flask, [Ir(phen) $_2$ OTf $_2$ ]OTf (86 mg, 0.086 mmol) and phenanthroline (31 mg, 0.172 mmol) were added successively. Then 10 mL 1,2-dichlorobenzene was added as solvent. The suspension was vacuumed and back-filled with argon then brought to reflux under argon for 12 hours. The mixture was cooled to room temperature to allow white solid to precipitate out of the yellow solution. The precipitate was filtered out and washed with chloroform and ether to afford the OTf salt of the target molecule as a white solid (65 mg, yield: 65%). The PF $_6$  salt was obtained by adding NH $_4$ PF $_6$  to an acetone solution of the OTf salt of the product. Then the suspension was filtered, and the filtrate was collected. After removal of the solvent, the residue was the desired PF $_6$  salt of the product.  $^1\text{H}$  NMR (400 MHz,  $\text{DMSO}-D_6$ ):  $\delta$  9.09 (dd,  $J$  = 8.4, 1.1 Hz, 6H), 8.55 (s, 6H), 8.13 (dd,  $J$  = 5.4, 1.1 Hz, 6H), 7.95 (dd,  $J$  = 8.3, 5.4 Hz, 6H). ESI-HRMS calcd for [C $_{36}$ H $_{24}$ IrN $_6$ ] $^{3+}$ : 244.3898; Found: 244.3893. Anal calcd (%) for C $_{39}$ H $_{24}$ IrN $_6$ S $_3$ O $_9$ F $_9$ •2H $_2$ O: C, 38.52; H, 2.32; N, 6.91. Found: C, 38.32; H, 2.57; N 7.08.

**Complex 2.** The similar procedure to the preparation of **1** was followed. Compounds [Ir(phen) $_2$ OTf $_2$ ]OTf (120 mg, 1.2 mmol) and phen-2F $_8$  (140 mg, 1.48 mmol) were added in 15 mL *o*-dichlorobenzene and the mixture was heated to 200 °C for 20 hours under argon. After the reaction mixture was cooled to room temperature, 100 mg of NH $_4$ PF $_6$  was added and the mixture was kept stirring for another 2 hours. The solvent was removed, and the crude product was purified by column chromatography (aluminum oxide gel) with CH $_2$ Cl $_2$ /MeOH = 20/1 (v/v) as the eluent to get the target complex as pale yellow solid (50 mg, yield: 21%).  $^1\text{H}$  NMR (400 MHz,  $\text{CDCl}_3$ ):  $\delta$  8.72-8.85 (m, 6H), 8.07-8.37 (m, 12H), 7.65-7.93 (m, 8H), 7.25-7.50 (m, 10H), 1.94-2.12 (m, 8H), 0.19-0.96 (m, 60H). ESI-HRMS calcd for [C $_{94}$ H $_{104}$ IrN $_6$ ] $^{3+}$ : 503.2654; Found: 503.2653. Anal calcd (%) for C $_{94}$ H $_{104}$ IrN $_6$ P $_3$ F $_{18}$ •2H $_2$ O: C, 56.99; H, 5.50; N, 4.24. Found: C, 57.29; H, 5.88; N 4.27.

**Complex 3.** In a 100-mL round bottle flask, *cis*-(phen) $_2$ RuCl $_2$ •2H $_2$ O (56.8 mg, 0.1 mmol), phenanthroline (18 mg, 0.1 mmol), and 20 mL ethanol were added. The reaction mixture was vacuumed and back-filled with argon for three times before it was brought to reflux for 24 hours. The red solution was cooled to room temperature and then 100 mg of NH $_4$ PF $_6$  was added. The mixture was further stirred at room temperature for 2 hours. Then the solvent was removed under reduced pressure and the residue was purified by column chromatography (silica gel) using CH $_2$ Cl $_2$ /MeOH = 40/1 (v/v) as the eluent to get the pure product as red solid (80 mg, yield: 80%).  $^1\text{H}$  NMR (400 MHz,  $\text{DMSO}-d_6$ ):  $\delta$  8.79 (d,  $J$  =

8.0 Hz, 6H), 8.39 (s, 6H), 8.09 (d,  $J = 5.2$  Hz, 6H), 7.76-7.80 (m, 6H). ESI-HRMS calcd for  $[\text{C}_{36}\text{H}_{24}\text{RuN}_6]^{2+}$ : 321.0558; Found: 321.0560. Anal calcd (%) for  $\text{C}_{36}\text{H}_{24}\text{RuN}_6\text{P}_2\text{F}_{12}$ : C, 46.41; H, 2.60; N, 9.02. Found: C, 46.14; H, 2.46; N 8.93.

**Complex 4.** The similar procedure to the preparation of **3** was followed. In a 100-mL round bottle flask, *cis*-(phen)<sub>2</sub>RuCl<sub>2</sub>•2H<sub>2</sub>O (37 mg, 0.06 mmol), phen-2F<sub>8</sub> (56 mg, 0.06 mmol), and 20 mL ethanol were added. The reaction mixture was vacuumed and back-filled with argon for three times before it was brought to reflux for 24 hours. The red solution was cooled to room temperature and then 100 mg of NH<sub>4</sub>PF<sub>6</sub> was added. The mixture was further stirred at room temperature for 2 hours, and then the solvent was removed under reduced pressure. The residue was purified by column chromatography (silica gel) using CH<sub>2</sub>Cl<sub>2</sub>/MeOH = 50/1 (v/v) as the eluent to get the desired complex as red solid (50 mg, yield: 50%). <sup>1</sup>H NMR (400 MHz, CDCl<sub>3</sub>):  $\delta$  8.42-8.55 (m, 8H), 8.09-8.22 (m, 6H), 7.89-7.92 (m, 4H), 7.54-7.81 (m, 6H), 7.27-7.47 (m, 12H), 1.91-2.09 (m, 8H), 0.25-0.94 (m, 52H), -0.04 (m, 8H). ESI-HRMS calcd for  $[\text{C}_{94}\text{H}_{104}\text{RuN}_6]^{2+}$ : 709.3696; Found: 709.3705. Anal calcd (%) for  $\text{C}_{94}\text{H}_{104}\text{RuN}_6\text{P}_2\text{F}_{12}\cdot\text{C}_6\text{H}_{14}$ : C, 66.91; H, 6.63; N, 4.68. Found: C, 66.94; H, 6.42; N 4.94.

### Photophysical Measurements

The spectroscopic grade solvents used for photophysical studies were purchased from VWR International and used without further purification. The ultraviolet-visible (UV-vis) absorption spectra were recorded on a Varian's Cary® 50 Spectrophotometer. Steady-state emission spectra were measured on a Jobin-Yvon FluoroMax-4 fluorometer/phosphorometer. The emission quantum yields were determined by relative actinometry method in degassed solvents, in which  $[\text{Ru}(\text{bpy})_3]\text{Cl}_2$  in degassed CH<sub>3</sub>CN ( $\lambda_{\text{max}} = 436$  nm,  $\Phi_{\text{em}} = 0.097$ )<sup>4</sup> was used as the reference for complexes **2-4**, and a 1 N sulfuric acid solution of quinine bisulfate ( $\lambda_{\text{ex}} = 347.5$  nm,  $\Phi_{\text{em}} = 0.546$ )<sup>5</sup> was used as the reference for complex **1**.

The nanosecond transient difference absorption (TA) spectra and decays were measured in degassed acetonitrile solutions on an Edinburgh LP920 laser flash photolysis spectrometer. The third harmonic output (355 nm) of a Nd:YAG laser (Quintel Brilliant, pulse width = 4.1 ns, repetition rate = 1 Hz) was used as the excitation source. Each sample was purged with argon for 45 min prior to measurement. The triplet excited-state absorption coefficients ( $\epsilon_{\text{T}}$ ) at the TA band maxima were determined by the singlet depletion method,<sup>6</sup> and the triplet excited-state quantum yield ( $\Phi_{\text{T}}$ ) was calculated by the relative actinometry,<sup>7</sup> in which SiNc in benzene was used as the reference ( $\epsilon_{590} = 70,000$  M<sup>-1</sup> cm<sup>-1</sup>,  $\Phi_{\text{T}} = 0.20$ ).<sup>8</sup>

### Computational Method

Geometry optimization of the complexes at their ground state, S<sub>0</sub>, was performed at the density functional theory (DFT) level using hybrid functional PBE1PBE.<sup>9</sup> The triplet excited state geometry, T<sub>1</sub>, was optimized using unrestricted DFT<sup>10</sup> within the same density functional as for the singlet structure calculations. All calculations were performed using mixed LANL2DZ basis set<sup>11</sup> for Ir(III) and Ru(II) and 6-31G\* basis set<sup>12-14</sup> for the ligands. Employing an effective core potentials (ECPs) basis such as LANL2DZ for transition metals, while using all-electron basis sets for all other non-transition-metal atoms has become a common practice in computations of metal-organic complexes.<sup>15</sup>

For absorption spectra calculations, we used linear response time-dependent DFT by iteratively solving the eigenvalue equation based on Davidson algorithm<sup>16-19</sup> applying the same density functional and the basis set as for the ground state calculations. For all complexes, 40 optical transitions,  $S_0 \rightarrow S_n$ , were included in the UV/Vis absorption spectra, plotted with inhomogeneous Gaussian line-broadening of 0.1 eV to reproduce the profile of the experimental spectra. The geometry optimization and optical absorption calculations were carried out in acetonitrile ( $\text{CH}_3\text{CN}$ ,  $\epsilon_r = 37.5$ ) solvent simulated by the conductor-like polarizable continuum model (CPCM).<sup>20,21</sup> All these calculations were performed using Gaussian 09 software package.<sup>22</sup>

The phosphorescence energy was calculated using a combined scalar relativistic ZORA and TDDFT approach<sup>21</sup> within the same functional and basis sets used for absorption spectra calculations. The phosphorescence calculations were also carried out in acetonitrile solvent, but using COSMO continuum solvation<sup>23,24</sup> model and NWChem software package.<sup>25</sup>

Natural transition orbital (NTO) analysis<sup>26</sup> was performed to obtain the orbitals of hole-electron pairs that contribute to each  $S_0 \rightarrow S_n$  optical transition, where a hole and an electron NTOs were obtained by the unitary transformation of transition density matrix of a given excited state. The lowest-energy triplet emitting state is obtained via the eigenvector analysis of the lowest excited state obtained from ZORA-TDDFT calculations and visualized by plotting the major contributing molecular orbitals. Chemcraft-1.7 software<sup>27</sup> was used for plotting the ground- and excited state charge densities using the isovalue of 0.02 for better visualization.

The energies of the  $e_g$  and  $t_{2g}$  orbitals of the Ir(III) and Ru(II) complexes were obtained by performing population analysis implemented in Gaussian09 software package. This was done by including the keyword "Pop = Orbitals" in the input file of the simulation. The atomic contribution ( $s$ ,  $p$  and  $d$  orbitals) to molecular orbitals was printed out at the end of the calculation, from which the highest occupied ( $t_{2g}$ ) and lowest unoccupied ( $e_g$ ) metal-based states are found. The orbital splitting energy was calculated by the energy differences between the  $e_g$  and  $t_{2g}$  orbitals.

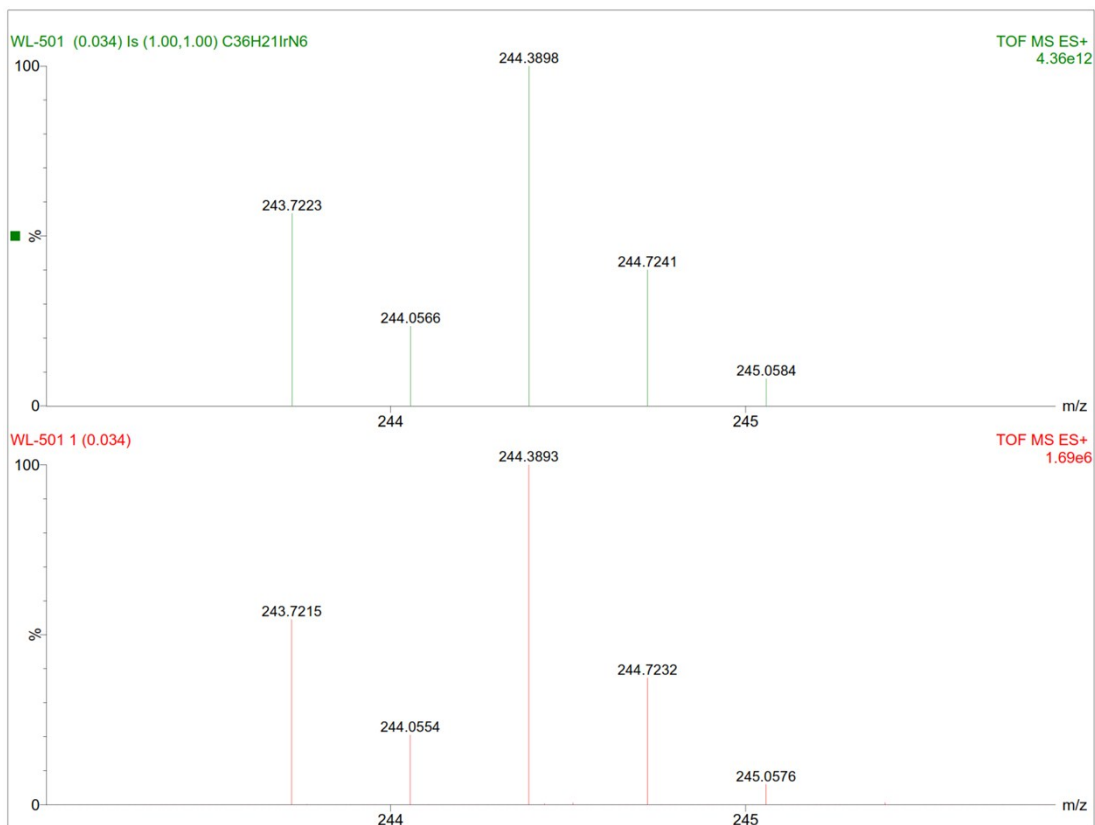
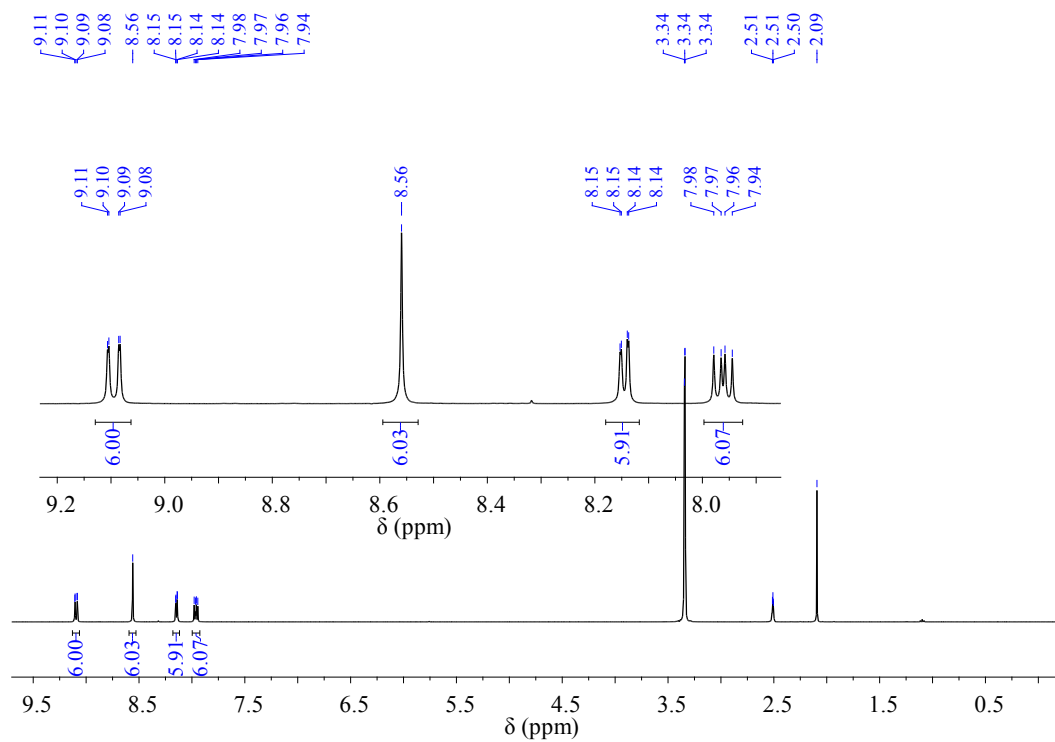


**Fig. S1**  $^1\text{H}$  NMR and HRMS spectra for complex **1**.

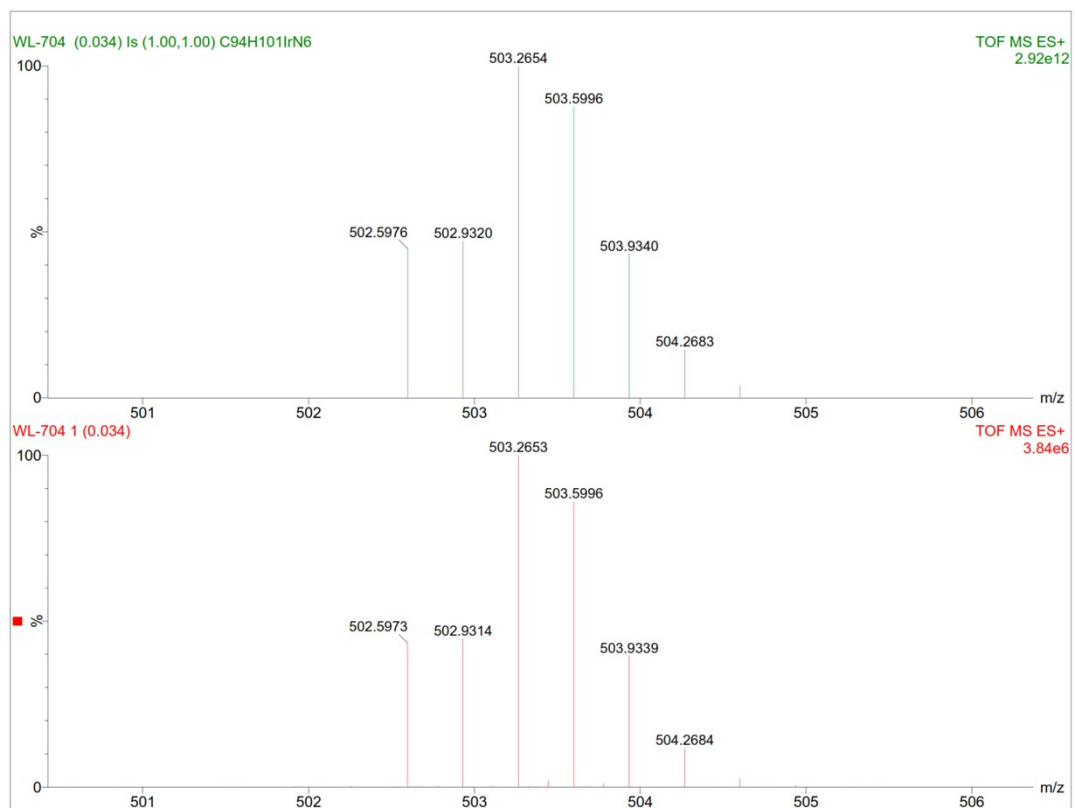
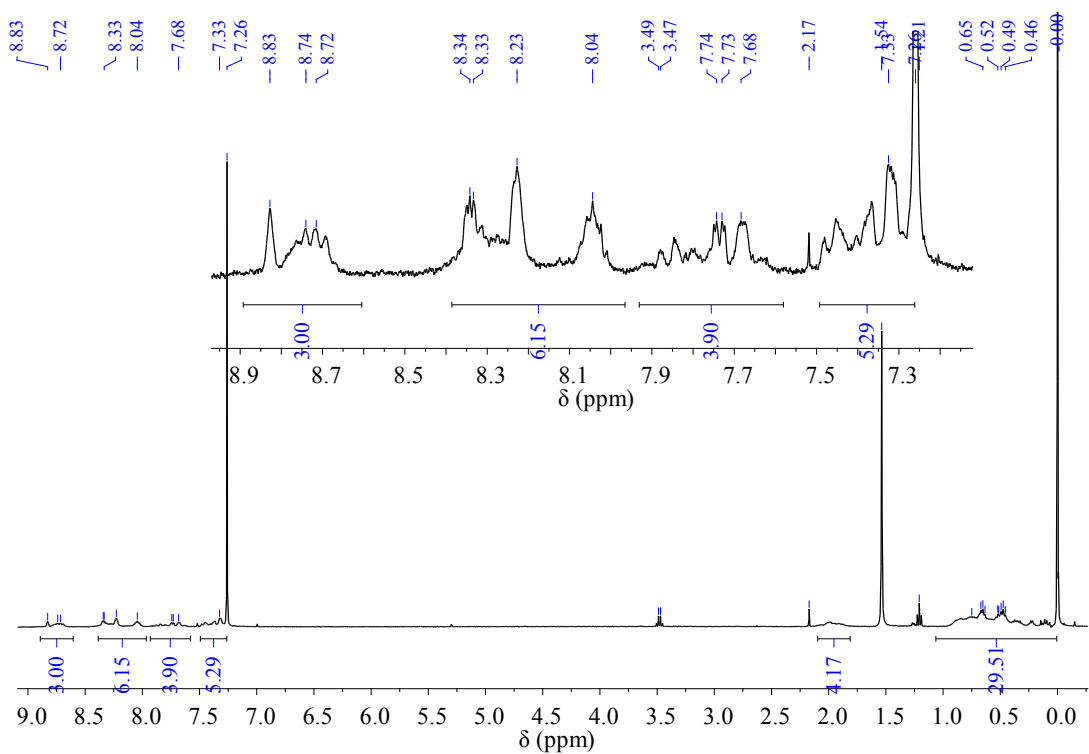


**Fig. S2** <sup>1</sup>H NMR and HRMS spectra for complex 2.

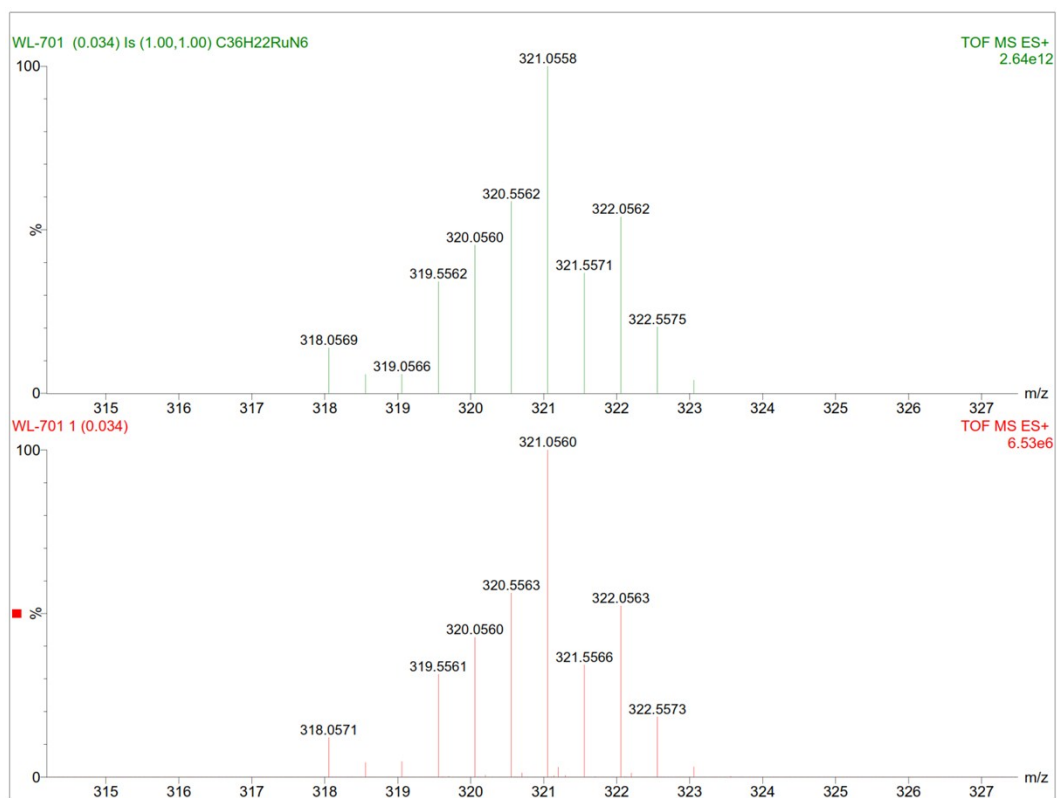
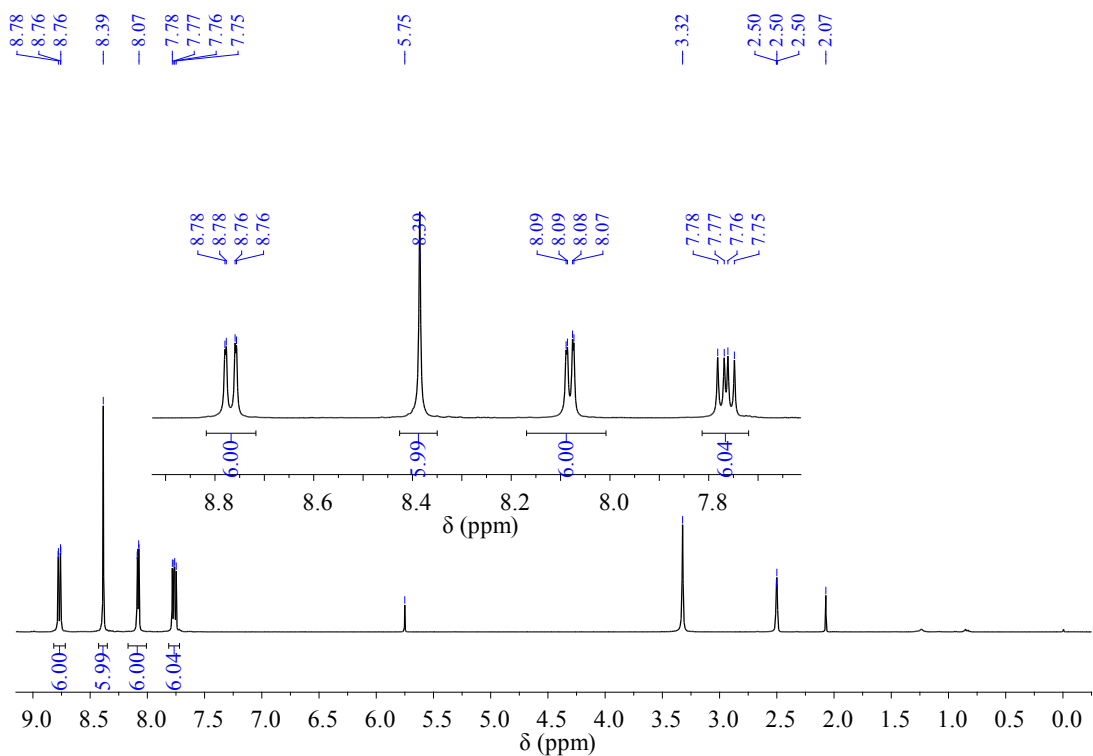
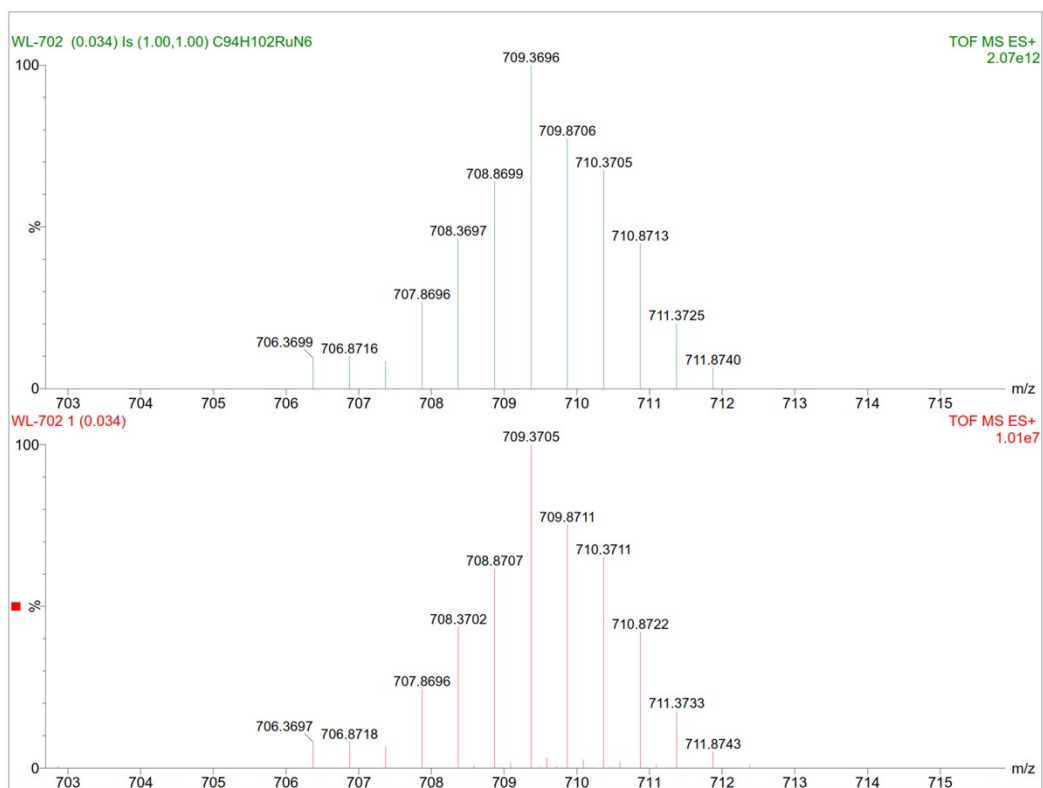
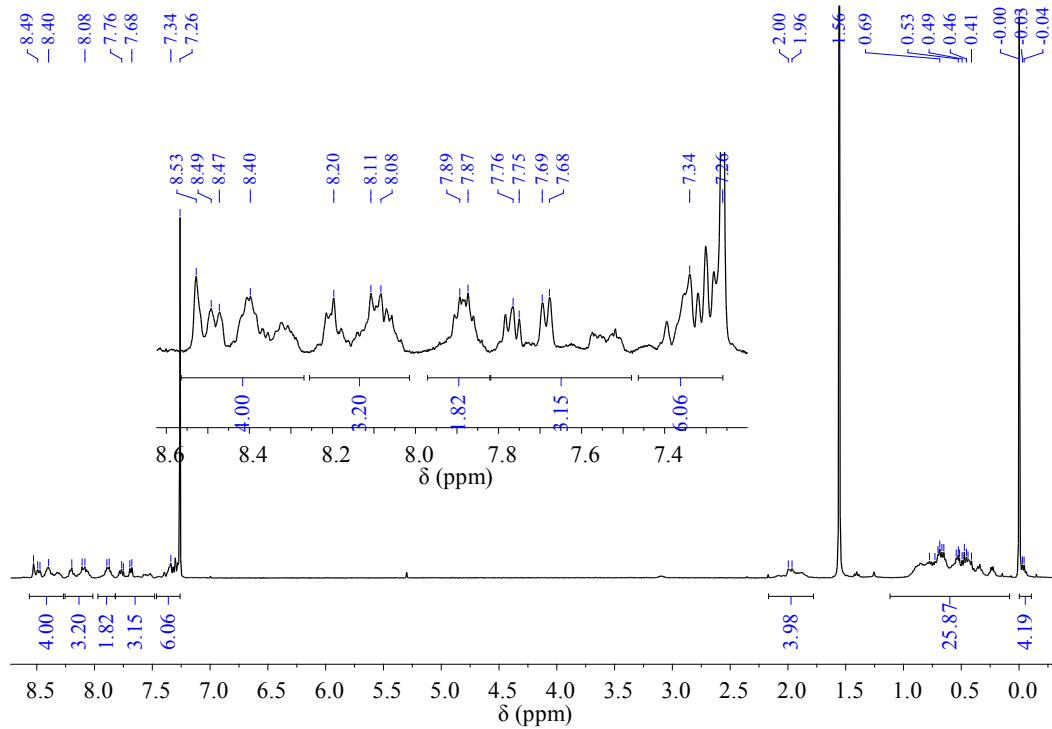
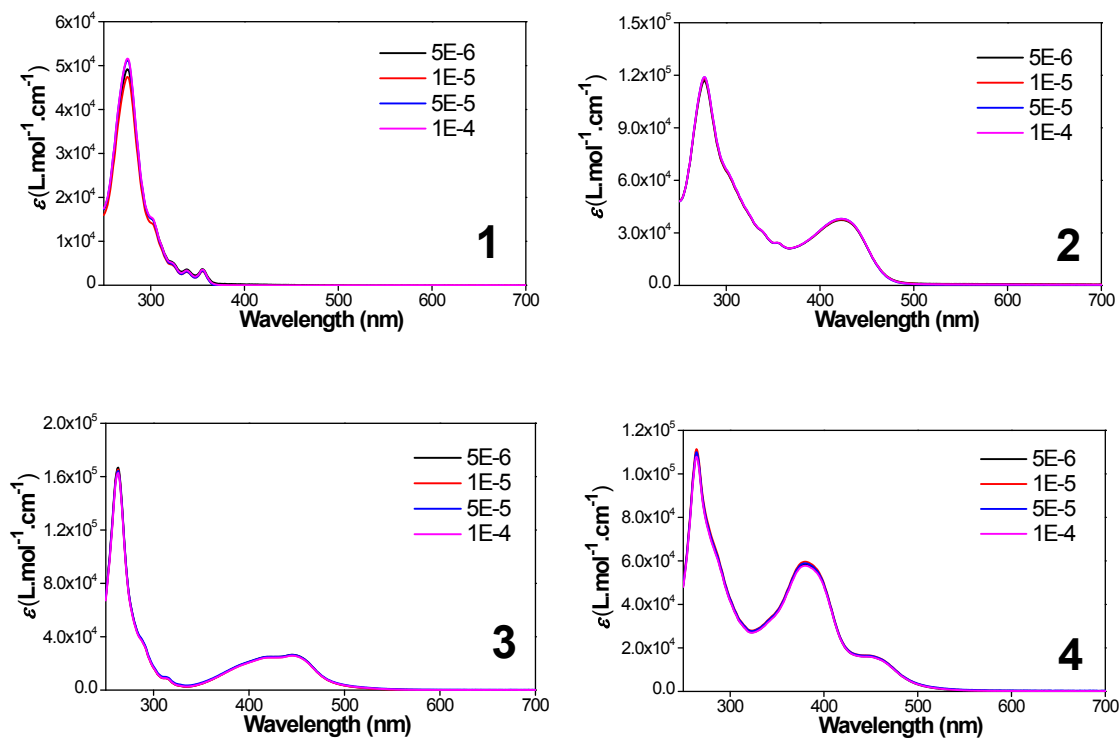


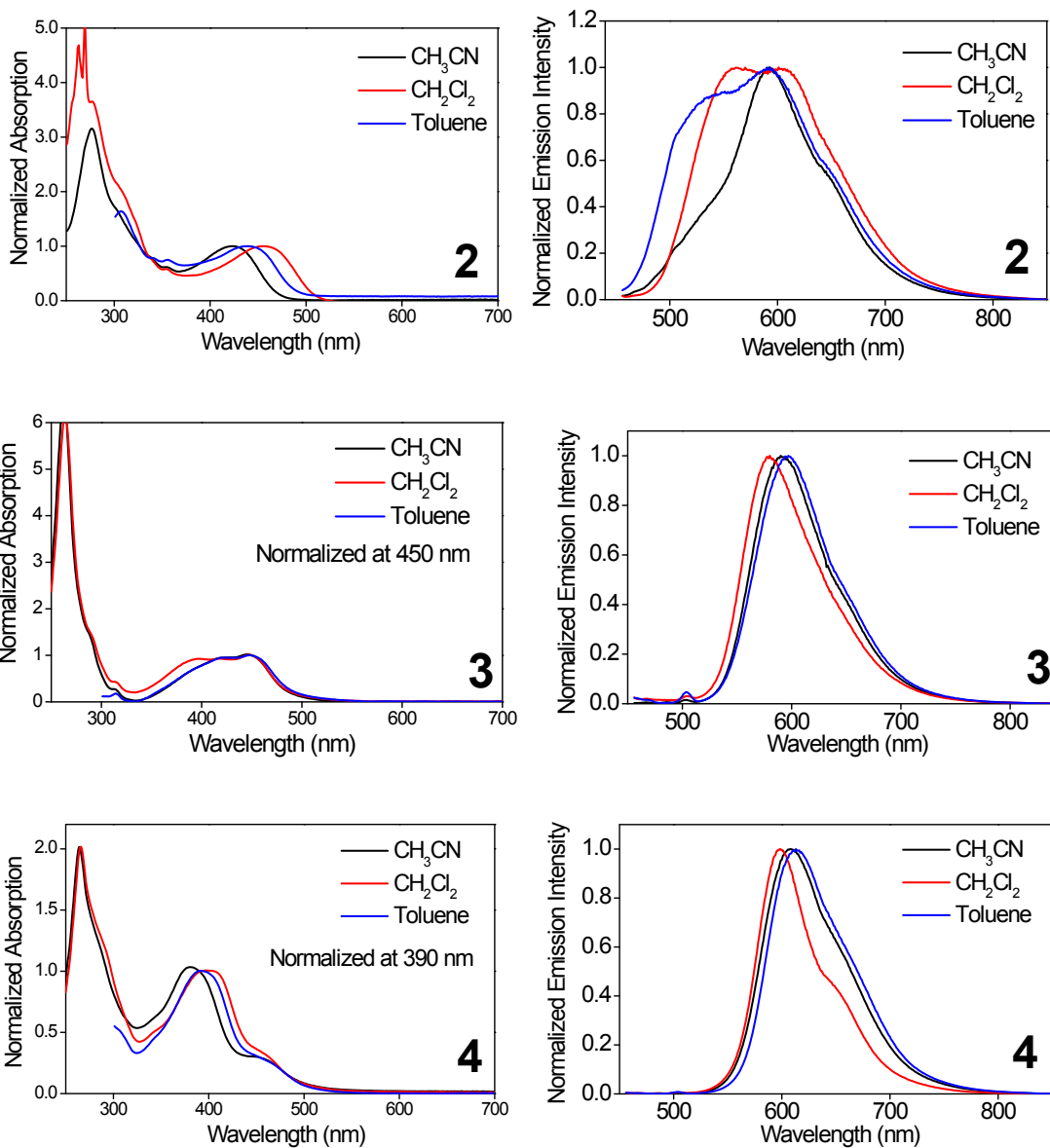
Fig. S3 <sup>1</sup>H NMR and HRMS spectra for complex **3**.



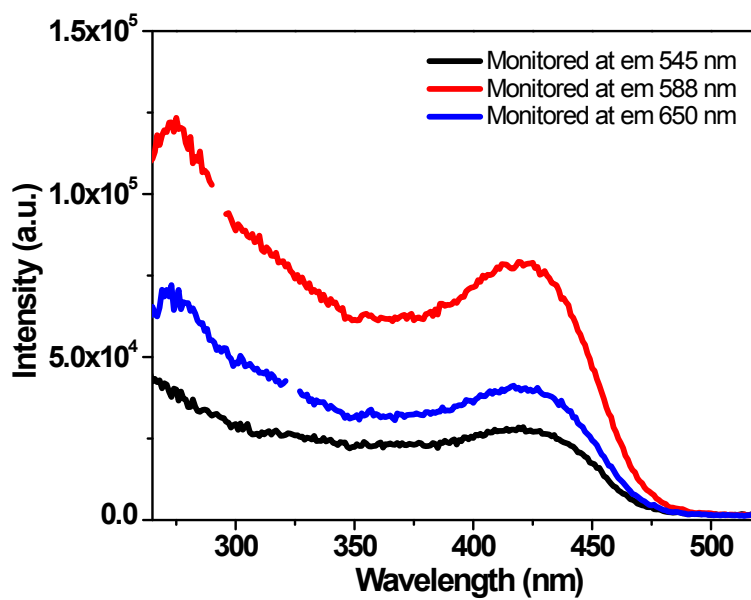
**Fig. S4** <sup>1</sup>H NMR and HRMS spectra for complex **4**.



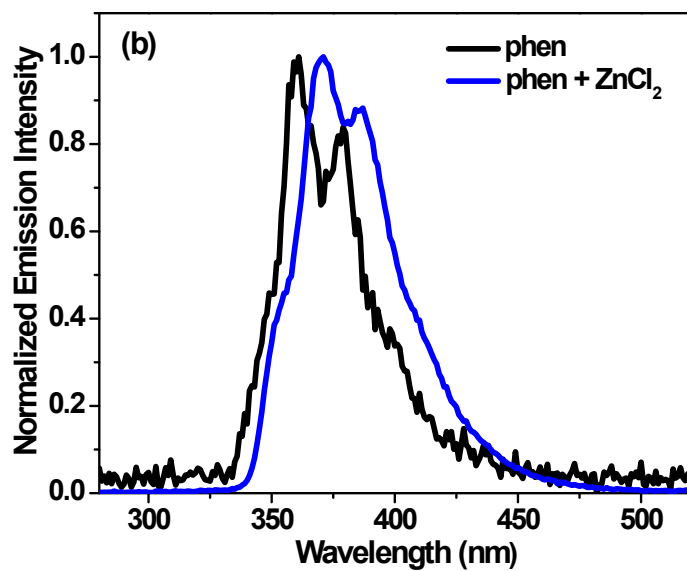
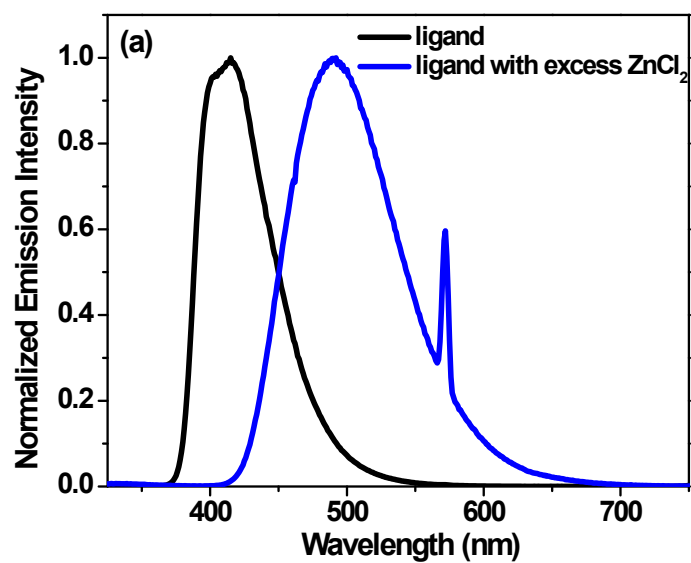
**Fig. S5** UV-vis absorption spectra for complexes **1-4** in acetonitrile at different concentrations at room temperature.



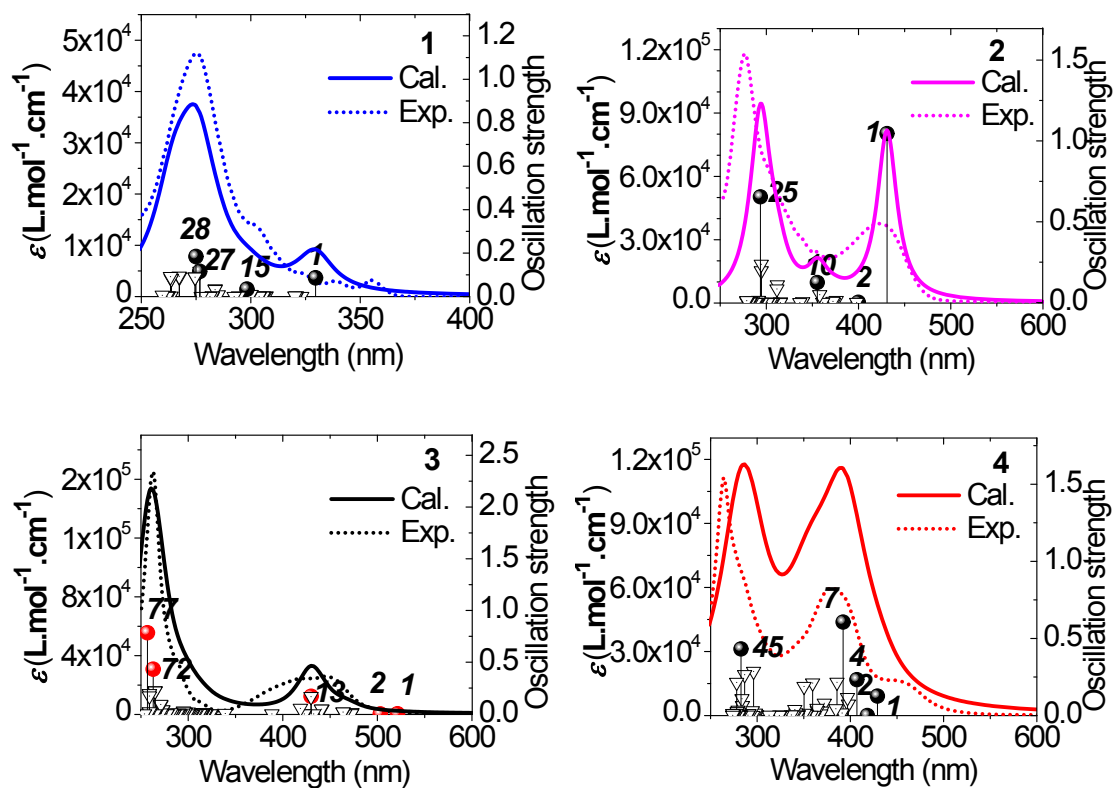
**Fig. S6** Solvent-dependency studies of UV-vis (left column) and emission spectra (right column) for **2** – **4** at room temperature ( $\lambda_{\text{ex}} = 436$  nm).



**Fig. S7** Excitation spectra of complex **2** in CH<sub>3</sub>CN monitored at different emission wavelengths.

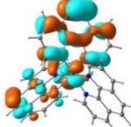
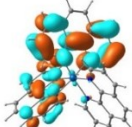
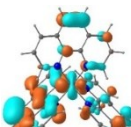
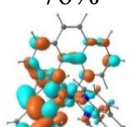
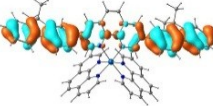
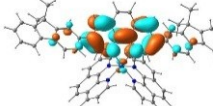
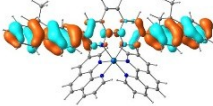
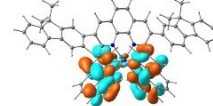
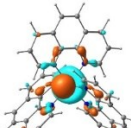
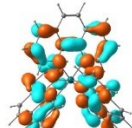
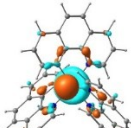
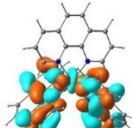
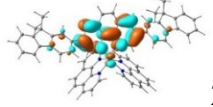
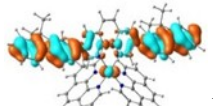
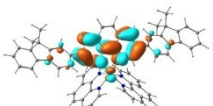
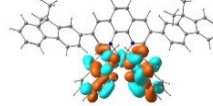
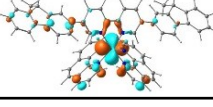
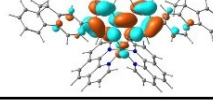


**Fig. S8** Fluorescence spectra of the fluorenyl substituted phen ligand (a) and the phen ligand (b) in CH<sub>3</sub>CN in the absence and presence of excess amount of ZnCl<sub>2</sub>.



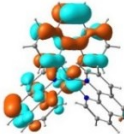
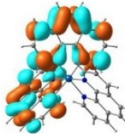
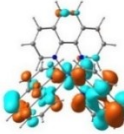
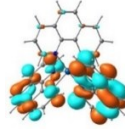
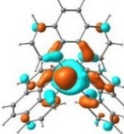
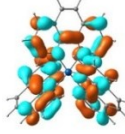
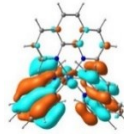
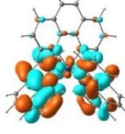
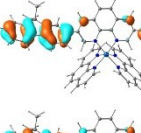
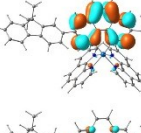
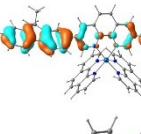
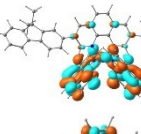
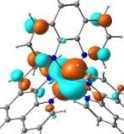
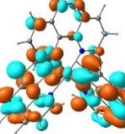
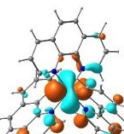
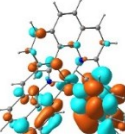
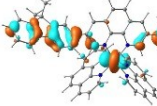
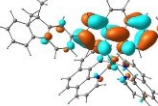
**Fig. S9** Comparison of the experimental and calculated UV-vis absorption spectra of complexes **1-4** in  $\text{CH}_3\text{CN}$ .

**Table S1.** Natural transition orbitals (NTOs) representing the lowest energy transitions for complexes **1-4** in CH<sub>3</sub>CN.

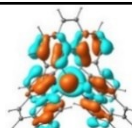
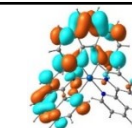
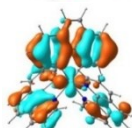
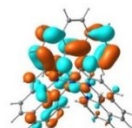
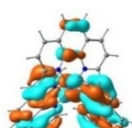
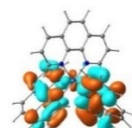
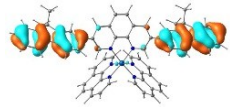
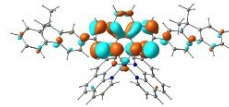
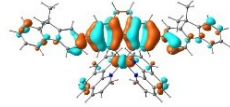
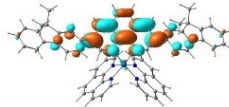
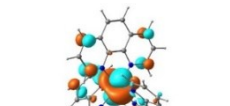
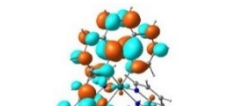
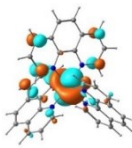
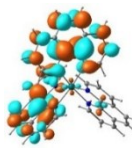
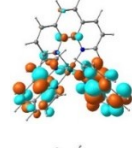
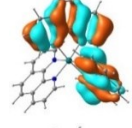
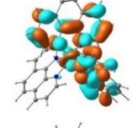
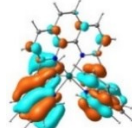
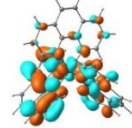
|          |  | HOTO   | LUTO   |
|----------|--|--|--|
| <b>1</b> | S <sub>1</sub><br>330 nm<br>$f = 0.09$<br>(H-L contribution (also major contribution): 30%)                      | <br>76%   | <br>76%   |
|          |  | <br>17%   | <br>17%   |
| <b>2</b> | S <sub>1</sub><br>433 nm<br>$f = 1.05$<br>(H-L contribution: 100%)<br>S <sub>2</sub><br>401 nm<br>$f = 0.003$    |          |           |
|          |  |          |           |
| <b>3</b> | S <sub>1</sub><br>521 nm<br>$f = 0.0016$<br>(H-L contribution: 100%)<br>S <sub>2</sub><br>503 nm<br>$f = 0.0001$ |          |          |
|          |  |         |         |
| <b>4</b> | S <sub>1</sub><br>429 nm<br>$f = 0.13$<br>(H-2→L contribution: 28%;<br>H-L contribution: 15%)                    | <br>28% | <br>28% |
|          |  | <br>15% | <br>15% |
|          | S <sub>2</sub><br>419 nm<br>$f = 0.0004$<br>S <sub>4</sub><br>407 nm<br>$f = 0.23$                               |        |         |
|          |  |        |         |



**Table S2.** Natural transition orbitals (NTOs) representing the main low-energy absorption and the main absorption bands for complexes **1-4** in CH<sub>3</sub>CN.

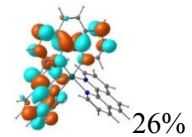
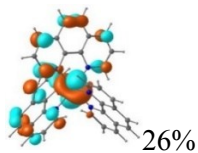
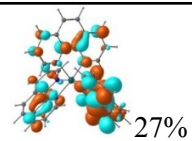
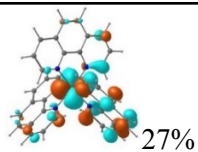
|          |  | HOTO  | LUTO  |
|----------|--|---|---|
| <b>1</b> | S <sub>15</sub><br>299 nm<br><i>f</i> = 0.03 |  26%   |  26%   |
|          |  |  23%   |  23%   |
|          |  |  26%   |  26%   |
|          |  |  23%   |  23%   |
| <b>2</b> | S <sub>10</sub><br>419 nm<br><i>f</i> = 0.16 |  77%  |  77%  |
|          |  |  23% |  23% |
| <b>3</b> | S <sub>13</sub><br>430 nm<br><i>f</i> = 0.17 |  68% |  68% |
|          |  |  27% |  27% |
| <b>4</b> | S <sub>7</sub><br>393 nm<br><i>f</i> = 0.61  |      |      |

**Table S3.** Natural transition orbitals (NTOs) representing the high-energy absorption bands for complexes **1-4** in CH<sub>3</sub>CN.

|          |                                  | Hole  | Electron  |
|----------|----------------------------------|---|---|
| <b>1</b> | $S_{27}$<br>277 nm<br>$f = 0.12$ |    |    |
|          |                                  |    |    |
|          |                                  | 28%   | 28%   |
|          |                                  |    |    |
|          |                                  | 27%   | 27%   |
| <b>2</b> | $S_{25}$<br>295 nm<br>$f = 0.65$ |  |  |
|          |                                  |  |  |
|          |                                  | 52%   | 52%   |
|          |                                  |  |  |
|          |                                  | 35%   | 35%   |
| <b>3</b> | $S_{72}$<br>263 nm<br>$f = 0.43$ |  |  |
|          |                                  |  |  |
|          |                                  | 27%   | 27%   |
|          |                                  |  |  |
|          |                                  | 26%   | 26%   |
| <b>4</b> |                                  |  |  |
|          |                                  | 12%   | 12%   |
|          |                                  |  |  |
|          |                                  | 12%   | 12%   |

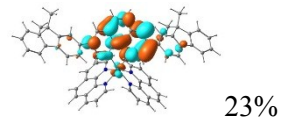
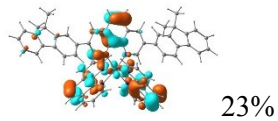
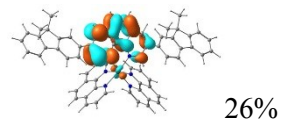
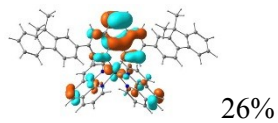
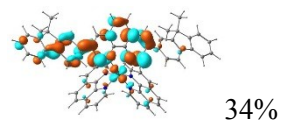
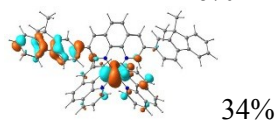
---

$S_{77}$   
257 nm  
 $f = 0.78$

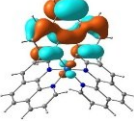
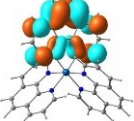
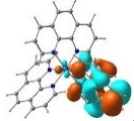
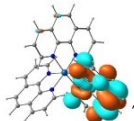
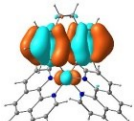
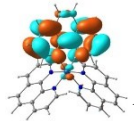
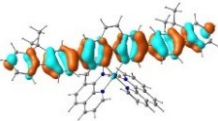
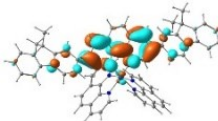
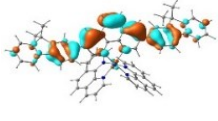
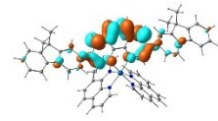
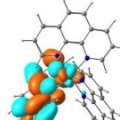
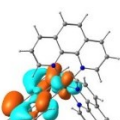
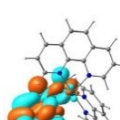
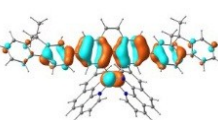
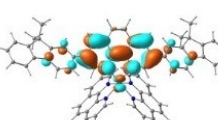
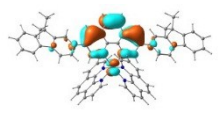
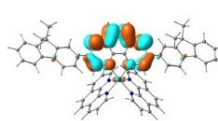


4

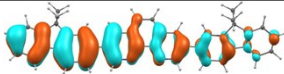
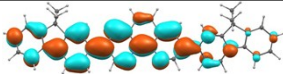
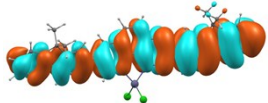
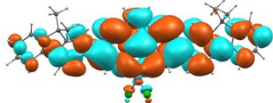
$S_{45}$   
283 nm  
 $f = 0.43$



**Table S4.** Molecular orbitals (MOs) corresponding to the phosphorescence emitting states of complexes **1-4** in CH<sub>3</sub>CN (Functional: PBE1PBE. Basis set: LANL2DZ/6-31G\*)

|          | Emission Energy | Occupied MOs  | Unoccupied MOs  |
|----------|-----------------|---|---|
| <b>1</b> | 452 nm          |  41%   |  41%   |
|          |                 |  24%   |  24%   |
|          |                 |  16%   |  16%   |
| <b>2</b> | 562 nm          |  82%   |  82%   |
|          |                 |  12%  |  12%  |
| <b>3</b> | 562 nm          |  83% |  83% |
|          |                 |  15% |  15% |
| <b>4</b> | 630 nm          |  84% |  84% |
|          |                 |  10% |  10% |

**Table S5.** Molecular orbitals (MOs) corresponding to the phosphorescence emitting states of the fluorenyl substituted phen ligand and its ZnCl<sub>2</sub> complex in CH<sub>3</sub>CN (Functional: PBE1PBE. Basis set: LANL2DZ/6-31G\*)

|                                     | Emission Energy | Occupied MO  | Unoccupied MO   |
|-------------------------------------|-----------------|--|---|
| Ligand                              | 701 nm          |  |  |
| ZnCl <sub>2</sub> Complex of Ligand | 703 nm          |  |  |

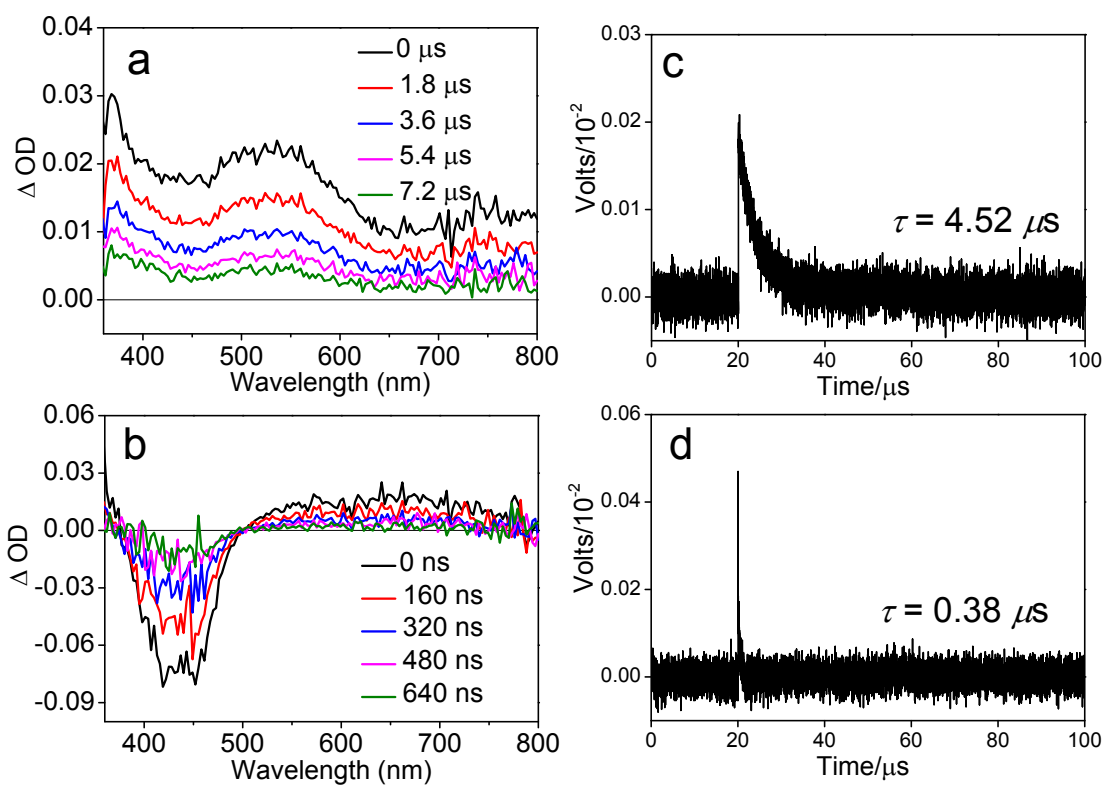


**Fig. S10** Time-resolved TA spectra and the decay curves at the respective TA band maxima for **1** (a, c) and **3** (b, d) in acetonitrile at room temperature.  $\lambda_{\text{ex}} = 355 \text{ nm}$ ,  $A_{355} = 0.4$  in a 1-cm cuvette.

## Reference

1. S. J. Slattery, N. Gokaldas, T. Mick and K. A. Goldsby, *Inorg. Chem.*, 1994, **33**, 3621-3624.
2. S. Soman, J. C. Manton, J. L. Inglis, Y. Halpin, B. Twamley, E. Otten, W. R. Browne, L. De Cola, J. G. Vos and M. T. Pryce, *Chem. Commun.*, 2014, **50**, 6461-6463.
3. X. Zeng, M. Tavasli, I. F. Perepichka, A. S. Batsanov, M. R. Bryce, C.-J. Chiang, C. Rothe and A. P. Monkman, *Chem. Eur. J.*, 2008, **14**, 933-943.
4. K. Suzuki, A. Kobayashi, S. Kaneko, K. Takehira, T. Yoshihara, H. Ishida, Y. Shiina, S. Oishi and S. Tobita, *Phys. Chem. Chem. Phys.*, 2009, **11**, 9850-9860.
5. W. H. Melhuish, *J. Phys. Chem.*, 1961, **65**, 229-235.
6. I. Carmichael and G. L. Hug, *J. Phys. Chem. Ref. Data.*, 1986, **15**, 1-250.
7. C. V. Kumar, L. Qin and P. K. Das, *J. Chem. Soc., Faraday Trans. 2*, 1984, **80**, 783-793.
8. P. A. Firey, W. E. Ford, J. R. Sounik, M. E. Kenney and M. A. J. Rodgers, *J. Am. Chem. Soc.*, 1988, **110**, 7626-7630.
9. C. Adamo and V. Barone, *J. Chem. Phys.*, 1999, **110**, 6158-6170.
10. I. Avilov, P. Minoofar, J. Cornil and L. De Cola, *J. Am. Chem. Soc.*, 2007, **129**, 8247-8258.
11. P. J. Hay and W. R. Wadt, *J. Chem. Phys.*, 1985, **82**, 270-283.
12. T. Clark, J. Chandrasekhar, G. W. Spitznagel and P. V. R. Schleyer, *J. Comput. Chem.*, 1983, **4**, 294-301.
13. M. M. Francl, W. J. Pietro, W. J. Hehre, S. Binkley, M. S. Gordon, D. J. DeFrees and J. A. Pople, *J. Chem. Phys.*, 1982, **77**, 3654-3665.
14. R. Krishnan, J. S. Binkley, R. Seeger and J. A. Pople, *J. Chem. Phys.*, 1980, **72**, 650-654.
15. Y. Yang, M. N. Weaver and K. M. Merz Jr., *J. Phys. Chem. A*, 2009, **113**, 9843-9851.
16. E. v. Lenthe, E.-J. Baerends and J. G. Snijders, *J. Chem. Phys.*, 1993, **99**, 4597-4610.

17. Casida, M. E, Recent Advances in Computational Chemistry: Volume 1. Recent Advances in Density Functional Methods (Part 1). D. P. Chong ed., 1995, **1**, 155-192.
18. L. Küne, L. Küne, *Z. Phys. Chem.*, 1998, **204**, 263-264.
19. R. Bauernschmitt and R. Ahlrichs, *Chem. Phys. Lett.*, 1996, **256**, 454-464.
20. M. Cossi, N. Rega, G. Scalmani and V. Barone, *J. Comput. Chem.*, 2003, **24**, 669-681.
21. V. Barone and M. Cossi, *J. Phys. Chem. A*, 1998, **102**, 1995-2001.
22. M. J. Frisch, G. W. Trucks, H. B. Schlegel, G. E. Scuseria, M. A. Robb, J. R. Cheeseman, G. Scalmani, V. Barone, B. Mennucci, G. A. Petersson, H. Nakatsuji, M. Caricato, X. Li, H. P. Hratchian, A. F. Izmaylov, J. Bloino, G. Zheng, J. L. Sonnenberg, M. Hada, M. Ehara, K. Toyota, R. Fukuda, J. Hasegawa, M. Ishida, T. Nakajima, Y. Honda, O. Kitao, H. Nakai, T. Vreven, Jr., J. A. Montgomery, J. E. Peralta, F. Ogliaro, M. Bearpark, J. J. Heyd, E. Brothers, K. N. Kudin, V. N. Staroverov, R. Kobayashi, J. Normand, K. Raghavachari, A. Rendell, J. C. Burant, S. S. Iyengar, J. Tomasi, M. Cossi, N. Rega, N. J. Millam, M. Klene, J. E. Knox, J. B. Cross, V. Bakken, C. Adamo, J. Jaramillo, R. Gomperts, R. E. Stratmann, O. Yazyev, A. J. Austin, R. Cammi, C. Pomelli, J. W. Ochterski, R. L. Martin, K. Morokuma, V. G. Zakrzewski, G. A. Voth, P. Salvador, J. J. Dannenberg, S. Dapprich, A. D. Daniels, Ö. Farkas, J. B. Foresman, J. V. Ortiz, J. Cioslowski and D. J. Fox, Gaussian 09, Revision A.1, Gaussian Inc., Wallingford, CT, USA, 2009.
23. D. M. York and M. Karplus, *J. Phys. Chem. A*, 1999, **103**, 11060-11079.
24. A. Klamt and G. Schuurmann, *J. Chem. Soc., Perkin Trans. 2*, 1993, 799-805.
25. M. D. Fayer, *Acc. Chem. Res.*, 2011, **45**, 3-14.
26. R. L. Martin, *J. Chem. Phys.*, 2003, **118**, 4775-4777.
27. G. Zhurko and D. Zhurko, URL: <http://www.chemcraftprog.com>, 2009.